Oestreicher and elastography

Edwin L. Carstensen[a] and Kevin J. Parker
Departments of Electrical & Computer and of Biomedical Engineering, University of Rochester, Rochester, New York 14627, USA

(Received 12 March 2015; revised 15 August 2015; accepted 31 August 2015; published online 22 October 2015)

A sphere moving back and forth in tissue generates the kinds of complex displacement fields that are used in elastography. The analytical solution of Hans Oestreicher for this phenomenon [(1951). J. Acoust. Soc. Am. **23**, 704–714] gives an understanding of the transverse and longitudinal, fast and slow waves that are generated. The results suggest several ways to determine the absorption coefficients of tissues, which together with phase velocity permit the computation of both the real shear modulus and the shear viscosity as functions of frequency.
 [http://dx.doi.org/10.1121/1.4930953]

[KAW] Pages: 2317–2325

I. INTRODUCTION

Long before the advent of elastography, Hans Oestreicher (Fig. 1) published a rigorous, analytical solution for the particle displacement field and impedance of a sphere, oscillating in translation in a viscoelastic medium (Oestreicher, 1951). His solution was for the steady state; his medium was linear and its stiffness and viscosity were coincident. Four decades later, the concept of elastography as a diagnostic tool was introduced. Since the turn of the century, there has been an explosion in relevant, theoretical and experimental research and instrument development. The current state of the field is summarized in recent reviews (Doherty *et al.*, 2013; Parker *et al.*, 2011; Sarvazyan *et al.*, 2013). Even today, however, careful inspection of Oestreicher's early work gives us valuable insight into the displacement fields that are used in all forms of elastography. His work gives us perhaps the simplest analytical model that involves all of the complex, free-field wave interactions that we have in the real world of elastography. The implied tissue shear strains that are potentially important in biological effects are discussed elsewhere (Carstensen *et al.*, 2015).

II. BASIC ASSUMPTIONS

For elastography, the fundamental, observable, physical quantity is the time-and-space-dependent particle displacement within the tissue of interest. Oestreicher, like many before him, assumed that the movements of particles in a medium obey Newton's second law of motion and that tissues act like a linear, homogeneous, isotropic viscoelastic (VE) media with coincident stiffness moduli and viscosities. This model gives order to what would otherwise be just a massive collection of displacement data. It predicts that the displacements pass their momentum to their neighbors in waves. The equation of wave motion can be split into two, one of which describes a fast wave dominated by the large bulk modulus κ with wave speeds on the order of 1500 m s^{-1} and the other, a slow wave related to the much smaller shear modulus μ with speeds in soft tissues between 1 and 10 m s^{-1}. Oestreicher solved these equations for the special case in which the source is a sphere translating harmonically.

Oestreicher's paper provides us with two, qualitatively different pictures of the interaction of the oscillating sphere with the surrounding medium: (1) the displacement fields that its movement generates in the medium and (2) the impedance that the sphere itself experiences. Each, in its own way, can give us information about the dynamic, mechanical properties of tissues.

Splitting the general wave equation into fast and slow parts defines each wave by its null characteristics, either zero curl or zero divergence—the fast wave is irrotational and the slow wave is incompressible. In a more positive view, we can have both transverse and longitudinal components of fast waves. They just cannot contribute to rotation. We can have longitudinal and transverse components of slow waves. They just cannot contribute to compression or bulk strain. And, both fast and slow waves can contribute shear strain. In fact, all strains of importance in elastography are shear. In

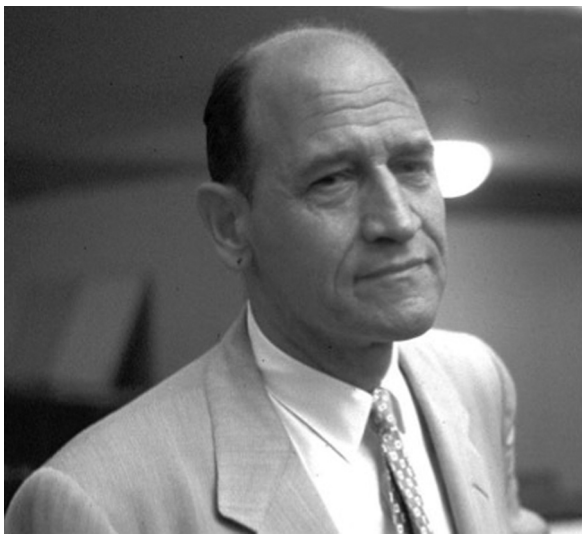

FIG. 1. Hans Oestreicher (1912–1995).

[a]Electronic mail: ecarsten@rochester.rr.com

principle, longitudinal displacements can contribute to bulk strain. However, at the frequencies used in elastography, those strains are many orders of magnitude smaller than the corresponding longitudinal shear strains as discussed elsewhere (Carstensen *et al.*, 2015). In effect, tissues are effectively incompressible for elastography applications.

Examples of transverse fast waves include the well-known, simple, acoustic dipole source. It is comprised of two purely longitudinal fast waves but has a fast (i.e., irrotational) transverse component as well as a fast longitudinal component (Morse and Ingard, 1987; Chanaud, 2010). Catheline and Benech (2015) treat the case of a translating point source. Like Oestreicher, they give their solution for the displacement field as the sum of a fast and a slow wave. The fast wave has both transverse and longitudinal components. In Oestreicher's treatment of the translation of a finite sphere in a viscoelastic solid, both slow and fast waves have components of displacement in the transverse (polar) directions and in the longitudinal (radial) directions. In sinusoidal steady state conditions, these components are simultaneously present and they can be of similar magnitudes. Elastography's displacement detectors have demonstrated the fast, longitudinal wave (Gennisson and Cloutier, 2006; Gennisson *et al.*, 2006). In principle, it should also be possible to detect the transverse component of the fast wave. We are not aware of an attempt to demonstrate it, however.

There are many advantages in the use of the wave approach for the measurement of the shear moduli of tissues and tissue phantoms. One only needs to determine the phase velocity and the absorption coefficient of the slow wave to compute the real and imaginary components of the effective complex shear modulus at a given frequency—no need for quantitative measurement of tissue strains or local stresses. The impedance, which the sphere experiences, is an alternate path that may reveal tissue properties under conditions in which no useful slow wave can be propagated.

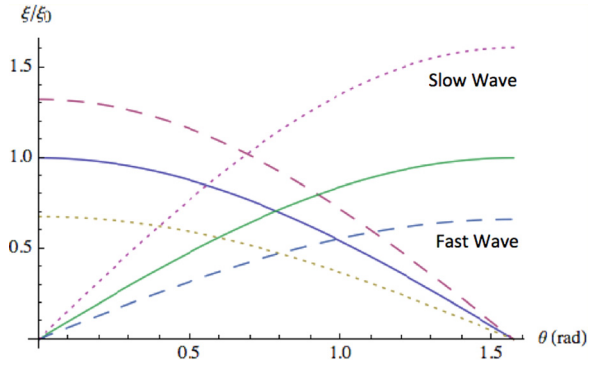

FIG. 2. (Color online) Absolute values of the radial (left) and tangential (right) components of the particle displacement at the surface of a sphere oscillating in translation. Solid curves are the net displacements whereas the fast wave and slow wave contributions are dashed and dotted, respectively. The tangential component (dotted curve) is in the direction of the negative of the unit $\vec{e}_\theta$ vector. The normalized displacement vector at the boundary is unity and directed along the axis of oscillation. $a = 0.01$ m, $\omega = 1000\,\mathrm{s}^{-1}$, $\mu_1 = 3$ kPa, $\mu_2 = 3$ Pa s, $\rho = 1000\,\mathrm{kg\,m}^{-3}$. Choosing $a = 1$ cm permits quantitative illustrations of general physical phenomena. Actual sources of interest may be much smaller (e.g., radiation force) or much larger (e.g., phantom studies).

III. THE DISPLACEMENT FIELDS

Oestreicher presented his solution as the sum of a fast wave and of a slow wave. Writing the sum in spherical coordinates emphasizes the longitudinal (radial) and transverse (polar) components of the total field. In spherical coordinates with the direction of the axis of oscillation along the zero polar angle, Oestreicher's solution for the displacement field of a sphere of radius a, translating harmonically with an amplitude ξ_0, becomes the sum of products of separate functions of radial position r, polar angle θ and time t,

$$\vec{\xi}(r,\theta,t) = \xi_0 e^{j\omega t}(\xi_r(r)\cos\theta\vec{e}_r + \xi_\theta(r)\sin\theta\vec{e}_\theta), \tag{1}$$

$\vec{e}_r$ and $\vec{e}_\theta$ being the radial and polar unit vectors and

$$\xi_r(r) = \frac{a^3}{r^3}\left(\frac{e^{-jk(r-a)}\left(3+3jha-(ha)^2\right)\left(-2-j2kr+(kr)^2\right)}{\left(2+2jka-(ka)^2\right)(ha)^2+(ka)^2(1+jha)} + \frac{e^{-jh(r-a)}2\left(3+3jka-(ka)^2\right)(1+jhr)}{\left(2+2jka-(ka)^2\right)(ha)^2+(ka)^2(1+jha)}\right), \tag{2}$$

$$\xi_\theta(r) = \frac{a^3}{r^3}\left(\frac{e^{-jk(r-a)}\left(3+3jha-(ha)^2\right)(1+jkr)}{\left(2+2jka-(ka)^2\right)(ha)^2+(ka)^2(1+jha)} - \frac{e^{-jh(r-a)}\left(3+3jka-(ka)^2\right)\left(1+jhr-(hr)^2\right)}{\left(2+2jka-(ka)^2\right)(ha)^2+(ka)^2(1+jha)}\right). \tag{3}$$

With the sphere oscillating along the $\theta = 0$ axis, $\xi_\phi(r) = 0$. Equation (1) satisfies the boundary conditions with a longitudinal displacement of $\vec{\xi}(a,0,t) = \xi_0 e^{j\omega t}\vec{e}_r$ and a transverse displacement of $\vec{\xi}(a,\pi/2,t) = -\xi_0 e^{j\omega t}\vec{e}_\theta$. The amplitude of the longitudinal component is proportional to $\cos\theta$ and the transverse component to $\sin\theta$.

ξ_r and ξ_θ each have a fast-wave term with a propagation constant $k = \omega/c_{f\phi}$, ω being the angular frequency and $c_{f\phi}$ the phase velocity of the fast wave, and a slow-wave term with a complex propagation constant $h = \omega/c_s = \beta - j\alpha$, where c_s is the slow wave speed, $\beta = \omega/c_{s\phi}$, $c_{s\phi}$ being the phase velocity of the slow wave and α its absorption coefficient. If bulk viscosity is comparable in magnitude to shear viscosity, its contribution is negligible at frequencies used in elastography and we may consider the fast propagation constant to be real. All of these components must add in such a

way that they give the real displacement at the surface of the sphere. If the phases of the solutions for the fast and slow waves differ at the source, it may require that one or both of the individual waves have amplitudes greater than the source (Fig. 2). A particle cannot simultaneously have two amplitudes and two phases, so the concept of a wave with amplitude greater than the source is a mathematical artifice.

Of course, the solution can be written as the sum of a fast and a slow wave as Oestreicher did. With a short pulse, fast and slow components separate spatially as they move away from the source and can be observed experimentally as in the case of transient elastography (Catheline *et al.*, 1999a; Catheline *et al.*, 1999b; Gennisson and Cloutier, 2006; Gennisson *et al.*, 2006; Oudry *et al.*, 2009; Sandrin *et al.*, 1999; Sandrin *et al.*, 2002). In that case, each of the pulses has a longitudinal and a transverse component. However, both fast and slow waves must coexist at the surface of the sphere, and their amplitudes are determined by boundary conditions there. Hence, the two waves are dependent even if they separate as pulses after leaving the sphere. Either way we choose to view the problem, there are waves traveling at fast ($\sim$1500 m s^{-1}) and slow (1–10 m s^{-1}) speeds throughout the medium, each with transverse as well as longitudinal components,.

The complete solutions [Eqs. (1)–(3)] have been used in all of our illustrations. For purposes of discussion, however, they can be simplified by noting that for conditions relevant to elastography, $ka < kr \ll 1$ and, in many cases, $hr > ha > 1$. We have used $a = 1$ cm for illustrations of the basic physical processes found in elastography. Except for the displacements at the surface of the sphere, precise numerical values for the displacement are a complicated interaction of the phases of fast and slow waves that in turn depend upon the tissue parameters and the frequency of oscillation. In a very general sense, increasing the size of the source sphere increases the displacement at a given point in the surrounding medium. Numerical methods would probably be needed for more precise predictions of the fields of practical sources used in a clinical setting. In the simplest applications, however, we learn that tissue is essentially incompressible but not rigid and that slow wavelengths are small compared to the region of interest in many tissues. With that simplification, Eqs. (2) and (3) become

$$\xi_r(r) \sim -\frac{a}{h^2 r^3}\left(3 + 3jha - (ha)^2 - 3e^{-jh(r-a)}(1 + jhr)\right), \tag{4}$$

$$\xi_\theta(r) \sim -\frac{a}{2h^2 r^3}\left(3 + 3jha - (ha)^2 - 3e^{-jh(r-a)}(1 + jhr - (hr)^2)\right). \tag{5}$$

This is the difficult playing field upon which elastography is forced to work. The first three terms in the parentheses in Eqs. (4) and (5) are from the fast wave and contain no useful information. The fast and slow waves, however, are of comparable magnitude and the presence of the fast wave can be a source of error in measurements of the slow wave propagation constant h, which contains the information that elastography seeks.

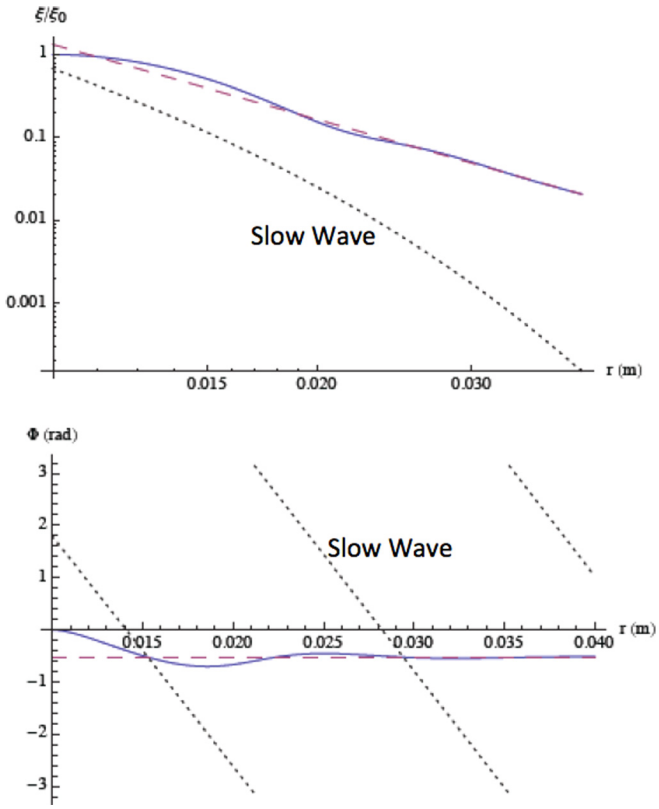

FIG. 3. (Color online) Absolute value of the normalized displacements and their phases along the axis of oscillation of the sphere. Total displacement (solid curves), fast wave contribution (dashed), and slow wave contribution (dotted). Values of the parameters used in Eq. (1) were chosen for their relevance to elastography. $a = 1$ cm, $\omega = 1000\,\mathrm{s}^{-1}$, $\rho = 1000\,\mathrm{kg\,m}^{-3}$, $\mu_1 = 3$ kPa, $\mu_2 = 3$ Pa s, $\kappa_1 = 2.2 \times 10^9$ Pa, $\kappa_2 = 0$, $\theta = 0$.

In the absence of viscous losses, the fast wave will attenuate as $1/r^3$ and the slow wave will fall as $1/r^2$ along the axis of oscillation, while at $\theta = \pi/2$, under optimum conditions, the lossless slow wave attenuates as $1/r$. One could call these lossless conditions the geometrical contributions to the attenuation. Tissues are far from lossless, of course. Realistic values of 3 kPa and 3 Pa s were used in Eq. (1) for the computation of the displacements presented in Figs. 3 and 4.

Several methods have been employed to measure $c_{s\phi}$ (and hence the real part of h) that do not require a precise knowledge of the amplitude of the wave. Transient elastography follows the crest of the slow wave along the axis of oscillation (Fig. 3) after it has separated from the fast wave. Echosens Fibroscan, the leading transient elastography system, operates at 50 Hz (Catheline *et al.*, 1999a; Catheline *et al.*, 1999b), while the frequency chosen for Fig. 3 is $\sim$150 Hz. Note that with the diagnostically relevant tissue properties chosen for Fig. 3, the fast wave dominates the displacement even near the source. Pulsing is essential, therefore, to separate fast and slow waves when the longitudinal wave is followed along the axis of oscillation.

The use of acoustic radiation force to generate displacement fields is particularly attractive because the source can be placed within the tissue itself and the displacement can be monitored along the $\theta = \pi/2$ axis, where the transverse wave is maximum and the geometrical attenuation of the slow wave goes as $1/r$ while the fast wave attenuates as $1/r^3$

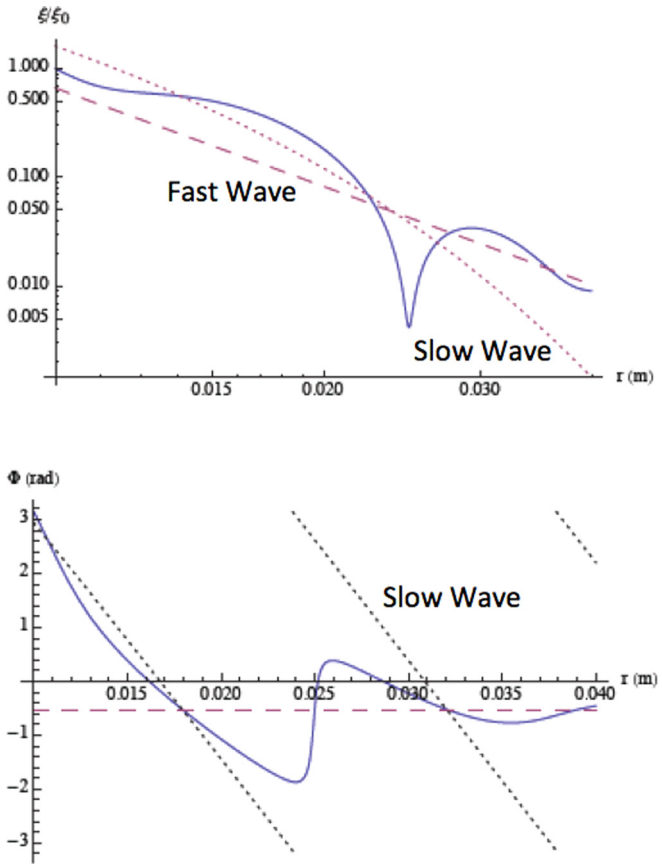

FIG. 4. (Color online) Absolute value of the normalized displacements and their phases along a radial line at $\theta = \pi/2$. Other values of the parameters used in Eq. (1) are the same as those used in Fig. 3.

(Fig. 4) (Sarvazyan *et al.*, 1998; Dahl, 2013). Most commercial devices at this writing use simple time of flight of the transverse slow wave as a function of distance giving it the group velocity, which is adequate for computation of clinically useful tissue stiffnesses (Palmeri *et al.*, 2008).

Several more sophisticated uses of radiation force sources are in the research and development stage. Chen *et al.* (2004) used amplitude modulation of a comparatively long radiation force pulse. Their results were limited to phase velocity of the displacement wave but, in principle, it should also be possible to determine the absorption. As noted above, absorption and phase velocity at a single frequency are sufficient to compute the effective VE shear modulus and shear viscosity. In fact, this has been done in a few studies (Catheline *et al.*, 2004; Gennisson and Cloutier, 2006; Gennisson *et al.*, 2006; Schmitt *et al.*, 2011; Urban and Greenleaf, 2009). The measurement of absorption is challenging (Domire *et al.*, 2009). Most investigators appear to find it easier determine shear viscosity through measurement of dispersion in velocity than to determine the absorption coefficient in tissue-like materials. That requires assumption that the viscosity is a simple, frequency-independent parameter. That may be a reasonable first order approximation. At the present time, a general investigation of the frequency dependence of the shear viscosity of tissues is lacking.

Urban, Chen and co-investigators (Urban *et al.*, 2009; Chen *et al.*, 2009) used a burst of very short radiation force pulses repeated at 100 Hz to generate a harmonic rich wave. Then they measured the phases of the waves at each harmonic at two different locations to determine the phase velocity spectrum—an efficient way to measure dispersion in phase velocity.

The figures, however, emphasize the difficulties faced in determining the phase velocity in the presence of the fast wave. MRE and sonoelastography experiments, for example, are typically performed with sinusoidal steady state conditions, so both fast and slow wave components would be superimposed. In the transverse wave (Fig. 4), the slow wave dominates and the fast wave may be ignored in phase velocity measurements near the source. As discussed below, it may be possible to extend phase velocity measurements by computing the rotation.

As currently practiced, elastography more or less ignores the fact that the response of tissue depends upon both its real shear modulus and its shear viscosity. Each of these parameters potentially has its own diagnostic information. Unfortunately, research on that subject is so limited that we can only speculate on the clinical value of shear viscosity. Mayo Clinic investigators used a form of modulated, ultrasound radiation force to measure dispersion in phase velocity in the livers of 10 normal volunteers and 35 patients that had been diagnosed with liver disease (Chen *et al.*, 2013). Taken as a whole, the data show a simply linear relationship between shear modulus and shear viscosity. The details, however, raise interesting questions. Whereas normal subjects were tightly clustered in a range 1.5–3 kPa and 1–3 Pa s, three out of 15 patients in early stage fibrosis had viscosities so high that they were classified as statistical outliers by the authors.

A qualitatively different study reports that slow waves propagating along muscle fibers are almost dispersionless while wave speed across the fibers are strong functions of frequency (Deffieux *et al.*, 2009), i.e., shear viscosity is almost qualitatively different in the same tissue depending upon the direction of propagation. Clearly, it would be unwise at this stage of our knowledge to write off viscosity as a possible diagnostic tool on its own. For that we need more than data fitting. Our tissue models must have their genesis in physical properties of the tissues.

Figure 5, using the same parameters chosen for Fig. 4, demonstrates the opportunities for absorption measurements with pulsed, transverse waves when the fast and slow components have been allowed to separate. Even with a conservative 3 Pa s value for μ_2, there is an order of magnitude decrease in the displacement within the distance of 1 cm. The dotted curve in Fig. 5 is the displacement for the slow transverse wave in a medium with an elastographically relevant 3 Pa s viscosity. The dash-dot curve is the geometrical $1/r$ displacement to be expected in the absence of viscous losses. As close as 3 cm from the source, the viscous absorption is two orders of magnitude greater than the geometrical contribution to the attenuation. It appears, therefore, that the viscosity can be measured at a single frequency with a precision limited only by the sensitivity of the displacement detector. The fast wave (dashed curve) would compromise absorption measurements in continuous wave fields. Similar

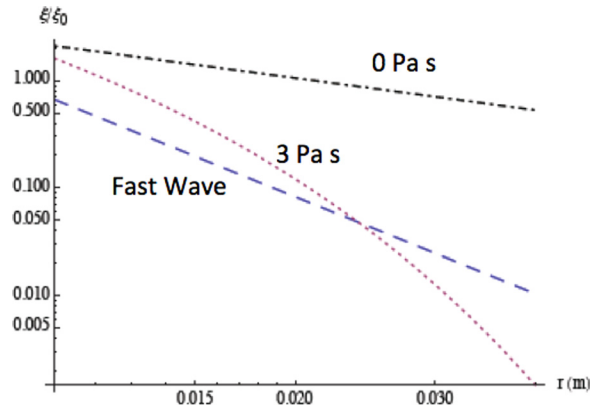

FIG. 5. (Color online) Contributions to the displacement of the fast and slow waves at $\theta = \pi/2$. The dashed curve is the normalized, absolute value of the fast wave. The dotted curve is for the slow wave with $\mu_2 = 3$ Pa s. The dash-dot curve gives the slow wave contribution under the assumption that $\mu_2 = 0$. All other parameters are as shown for Fig. 3.

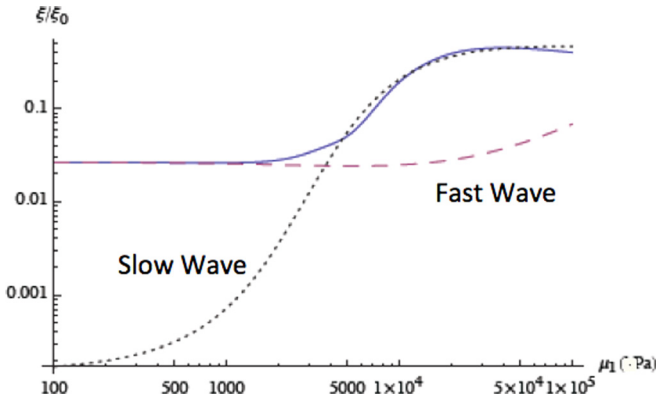

FIG. 6. (Color online) Particle displacement as a function of real shear modulus. Shown are the fast (dashed) and slow (dotted) contributions to the net transverse displacement (solid). $\theta = \pi/2$, $a = 1$ cm, $r = 3$ cm, $\omega = 1000\,\mathrm{s}^{-1}$, $\mu_2 = 3$ Pa s.

measurements would be possible along the axis of oscillation. However, the geometrical attenuation of the slow wave along that path goes as $1/r^2$ and is therefore potentially a greater source of error in absorption measurements.

IV. SENSITIVITY OF PARTICLE DISPLACEMENT TO TISSUE PARAMETERS

The amplitude of the displacement in the transverse slow wave is a very strong function of the real shear modulus under conditions relevant to elastography. Figure 6 gives a specific example of the high sensitivity of the slow wave to the shear modulus. In a more general sense, it demonstrates the dominant role that the fast wave can have and the need to consider that fact in practical elastography.

In principle, absorption measurements would be greatly simplified if we were able to use plane transverse waves. In that case, we would have neither "geometrical" attenuation nor a fast wave to complicate interpretation of our observations. One might conjecture that increasing the size of the source would minimize those factors. However, it turns out that unrealistically large sources would be required to significantly reduce the complexity of elastographic displacement fields. For example, the fast wave at $\theta = \pi/2$ is not significantly reduced until the radius of the sphere is on the order of the fast wavelength. Thus, we must live with the fact that realistic fields will always have complex combinations of transverse and longitudinal, fast and slow waves.

One final note that could be useful in absorption measurement techniques. Rotation, the anti-symmetric part of the second order, vector displacement gradient, is determined entirely by the slow wave component of the displacement. The fast (irrotational) wave contributes nothing to the rotation. Thus, by computing the rotation from displacement measurements, all effects of the fast wave are eliminated even in continuous wave measurements. (Sinkus *et al.*, 2005; Doyley, 2012). Figure 7 shows the strong dependence of the rotation on the viscous absorption. Rotations might potentially be useful for the measurement of viscosities as high as 10 Pa s at frequencies on the order of 1000 rad s^{-1} ($\sim$150 Hz).

V. IMPEDANCE

Oestreicher defined the impedance of a translationally oscillating sphere as the ratio of the force that the sphere exerts on the medium surrounding it to its translational velocity. His Eq. (18) gives the impedance

$$Z = -j\omega\frac{4}{3}\pi a^3\rho\frac{\left(1-j\frac{3}{ah}-\frac{3}{(ah)^2}\right)-2\left(j\frac{1}{ah}+\frac{1}{(ah)^2}\right)\left(3-\frac{(ak)^2}{1+jak}\right)}{\left(j\frac{1}{ah}+\frac{1}{(ah)^2}\right)\frac{(ak)^2}{1+jak}+\left(2-\frac{(ak)^2}{1+jak}\right)}. \tag{6}$$

So defined, Oestreicher's impedance tells us a great deal about the medium. As illustrated in Fig. 8, the system, at low frequencies, is quasi-static and the force required to displace the sphere is balanced by elastic forces (the stiffness of the medium). At high frequencies where mass dominates the motion, the force required to move the sphere will depend upon the density of the medium as well as the viscous properties of the tissue that it moves. For this discussion, we shall

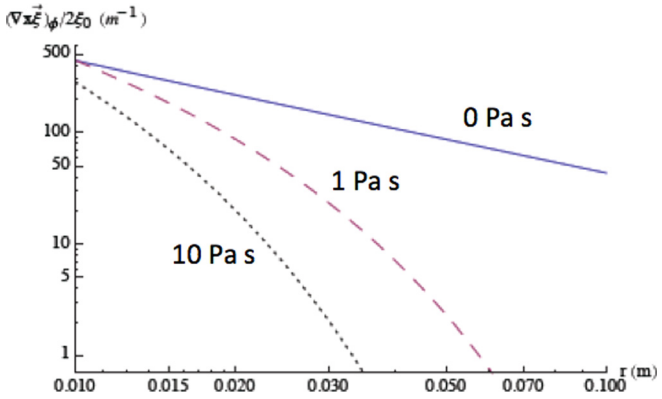

FIG. 7. (Color online) Absolute value of the rotation. $\mu_2 = 0$ Pa s (solid), $\mu_2 = 1$ Pa s (dashed), $\mu_2 = 10$ Pa s (dotted), $a = 1$ cm, $\omega = 1000\,\mathrm{s}^{-1}$, $\rho = 1000\,\mathrm{kg\ m}^{-3}$, $\mu_1 = 3$ kPa, $\theta = \pi/2$, and $k = 0$.

concentrate only on the sphere-medium interaction and ignore the additional force needed to move the sphere. However, in experimental studies using Oestreicher's impedance, it is necessary to take that omission into account (Chen *et al.*, 2002; Urban *et al.*, 2011).

At frequencies used in elastography, the motion of a sphere in tissue is controlled almost completely by the shear modulus of the medium, i.e., tissue is effectively an incompressible elastic solid ($k \sim 0$) and

$$Z \sim -j\omega\frac{2}{3}\pi a^3\rho\left(1 - j\frac{9}{ah} + \frac{3}{(ah)^2}\right). \tag{7}$$

With typical values for soft tissue parameters, Eqs. (6) and (7) agree to within 2% up to ~100 krad s^{-1}. Beyond that frequency, the bulk properties of the medium take over and the impedance tells us little about the slow wave parameters.

Measuring amplitude and phase of the impedance at a single frequency gives us the information we need to compute the real shear modulus and the shear viscosity at that frequency. It would be challenging to use these concepts in the clinical setting. However, laboratory studies with excised tissue should present few problems. In contrast with most elastography techniques, the determination of tissue properties through measurements of this impedance requires the absolute value of the driving force. Fortunately however, as shown in Eq. (7), there is insignificant interference from the presence of the fast wave—as there can be in continuous wave elastography.

At high frequencies ($\omega = 10^4$ to 10^5 rad s^{-1}) with a modest viscosity, Eq. (6) reduces to

$$Z \to -j\omega\frac{2}{3}\pi a^3\rho. \tag{8}$$

Under those conditions, the mass of the medium sets an upper limit to the motion. Its elastic properties are irrelevant.

At low frequencies, the shear modulus of the medium controls the motion of the sphere, i.e.,

$$Z \sim -j\frac{2\pi a\mu_1}{\omega}. \tag{9}$$

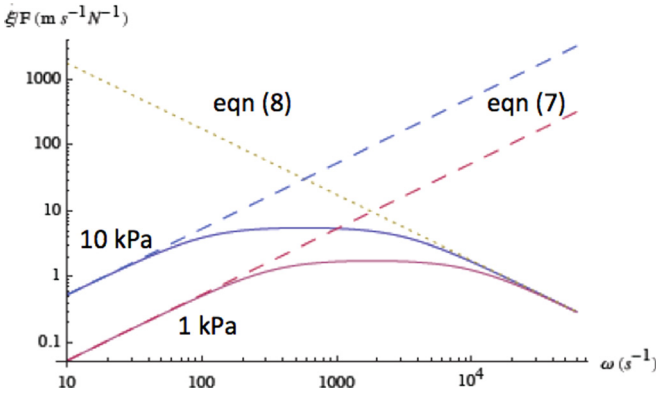

FIG. 8. (Color online) Absolute value of the translational velocity $\dot{\xi}$ of a 3 mm (radius) sphere driven by a force F. The solid curves are the predictions of Eq. (6). The upper curve is for $\mu_1 = 1$ kPa and the lower curve for $\mu_1 = 10$ kPa. The dotted line is the mass-dominated high frequency limit [Eq. (8)] and the dashed lines are the corresponding stiffness-dominated, low frequency limits [Eq. (9)]. Viscosity is assumed to be zero and the density of the medium is 1000 kg m^{-3}.

The intersection of Eqs. (10) and (11) gives the frequency ω_t of transition between stiffness and mass control, at which the normalized velocity reaches its maximum,

$$\omega_t = \frac{1}{a}\sqrt{\frac{3\mu_1}{\rho}}. \tag{10}$$

The essence of Eqs. (6) and (7) is shown in Figs. 8–11. The data are presented in terms of the velocity amplitude (the absolute value of the velocity) of the sphere normalized to the force that it exerts on the surrounding tissue and the phase of the velocity relative to the source force. These are likely to be the observables in experimental studies, although there would be advantages to direct measurements of displacement at very low frequencies. Figures 8 and 9 assume negligible viscosity. Figures 10 and 11 show the effects of viscosity on the admittance of the sphere. The large effects of viscosities comparable in magnitude to those of tissues on both the amplitude and the phase of the velocity of the sphere bode well for the use of impedance in the measurement of tissue viscoelastic properties. From our limited

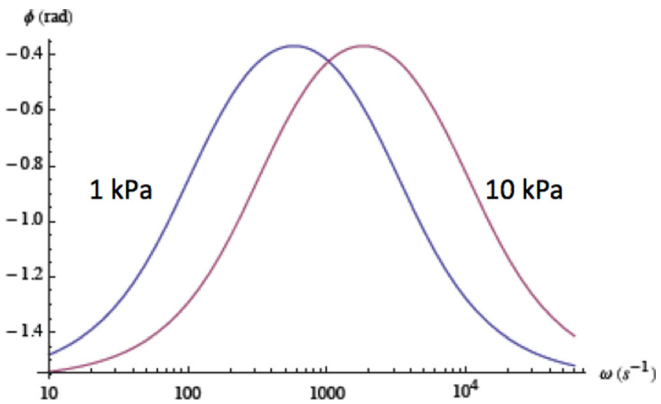

FIG. 9. (Color online) Phase of the velocity relative to driving force. Conditions are as listed in Fig. 8. $\phi = \arctan\,[\mathrm{Im}(\dot{\xi}/F)/\mathrm{Re}(\dot{\xi}/F)]$. On the left, $\mu_1 = 1$ kPa, on the right $\mu_1 = 10$ kPa.

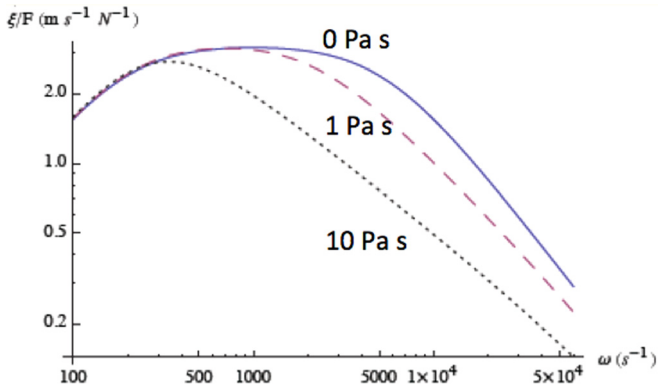

FIG. 10. (Color online) The normalized, absolute value of the translational velocity $\dot{\xi}$ of a sphere showing the influence of viscosity. $\mu_2 = 0$ (solid), $\mu_2 = 1$ Pa s (dashed), $\mu_2 = 10$ Pa s (dotted), $\mu_1 = 3$ kPa, $a = 3$ mm.

knowledge of the frequency dependence of the viscosity (Carstensen and Parker, 2014), we can be confident that actual measurements of tissues will give results somewhat different than the examples presented here. As with Oestreicher, we have assumed in these examples that both real shear modulus and the shear viscosity are simple constants, independent of frequency. Impedance could give the effective viscosity at the measurement frequency and thus the frequency dependence of the tissue parameters.

In principle, when the viscosity is very large, the impedance becomes $Z \rightarrow 6\pi a\mu_2$, the impedance of sphere of radius a in a viscous fluid. Viscosity dominance to that extent, however, requires viscosities an order of magnitude greater than those thus far reported for tissue. Instead, Figs. 10 and 11 show the effects of viscosities that are more realistic for soft tissue. It appears that the impedance experienced by the sphere will provide information about tissue viscosity at somewhat higher frequencies than would be possible with slow wave propagation.

The impedance approach should have certain potential advantages over wave propagation methods for studies of the shear properties of tissues. At high frequencies, slow waves simply do not propagate because of losses. Yet, as shown in Figs. 10 and 11, the impedance method becomes sensitive to viscosity in that region. At low frequencies, the impedance is strongly dependent upon the real shear modulus. But, at very low frequencies, the wavelengths of slow waves in achievable tissue samples become so large that wave motion is difficult to observe with precision. The normalized, displacement amplitude of a small sphere in the medium, however, is directly proportional to the real shear modulus in the low frequency limit.

Linear hysteresis probably contributes to loss in tissues and its diagnostic contributions may vary with pathology (Carstensen and Parker, 2014). Defined as a frequency independent loss per cycle or a frequency independent phase between displacement and stress (Mason, 1950), linear hysteresis has been formalized as $\mu = \mu_1 + j\mu_3$, where μ_3 is the hysteresis modulus to distinguish it from shear viscosity, which we have called μ_2. For any realistic tissue, we also have viscosity, so the complex shear modulus would be

$$\mu = \mu_1 + j(\omega\mu_2 + \mu_3), \tag{11}$$

from which we can see that hysteresis, if present, will be most strongly evident at low frequencies. As noted above, that may rule out wave studies for the investigation of hysteresis. Quasistatic elastography suggests that muscle is hysteretic while gels are not (Greenleaf *et al.*, 2003).

At low frequencies, losses in tissues are likely to be small whether from viscosity or hysteresis. The small absorptions and large wavelengths that make wave measurements problematic at low frequencies can actually be an advantage with impedance measurements. Although magnitudes of the impedance with the two mechanisms are apt to be similar at very low frequencies, the phase of the displacement of a small sphere relative to the driving force gives us a tool to differentiate between viscosity and hysteresis (Fig. 12). Our knowledge of hysteresis in tissues is extremely limited. However, if by hysteresis we mean frequency-independent phase lag, phase can be determined directly with elastographic technology—no need for absolute measurements of displacement.

At very low frequencies, slow wavelengths are large, i.e., the phase of the displacements relative to the driving force will be relatively uniform over large regions of tissue. This would permit phase determinations from measurements of the phase of tissue displacement at significant distances from the source. In this way, phase measurements similar to

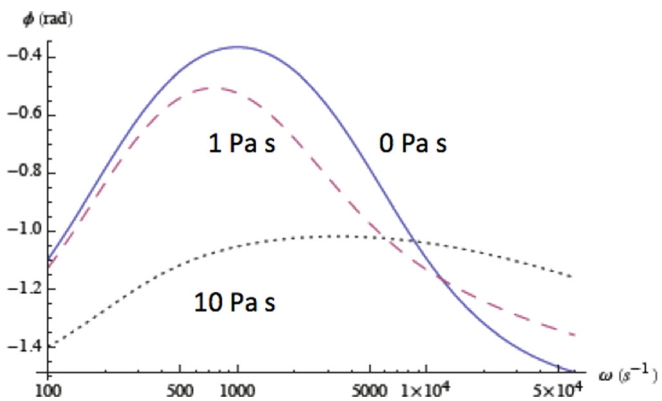

FIG. 11. (Color online) Phase of the velocity relative to driving force. Conditions are as listed in Fig. 10. $\phi = \arctan\,[\mathrm{Im}(\dot{\xi}/F)/\mathrm{Re}(\dot{\xi}/F)]$.

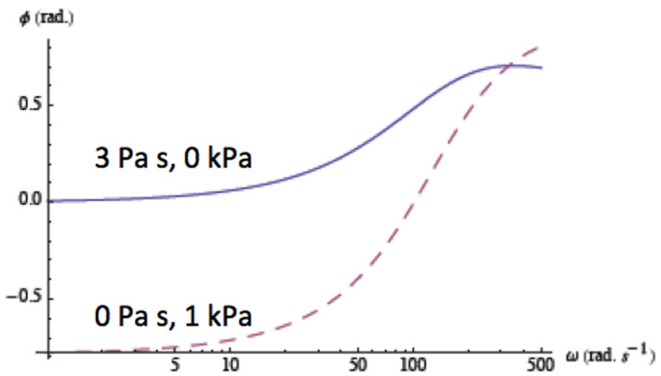

FIG. 12. (Color online) Phase of 3 mm sphere relative to driving force. The solid curve assumes a viscosity of 3 Pa s and zero hysteresis; the dashed curve is for $\mu_3 = 1$ kPa and zero viscosity. $\mu_1 = 1$ kPa, $a = 3$ mm.

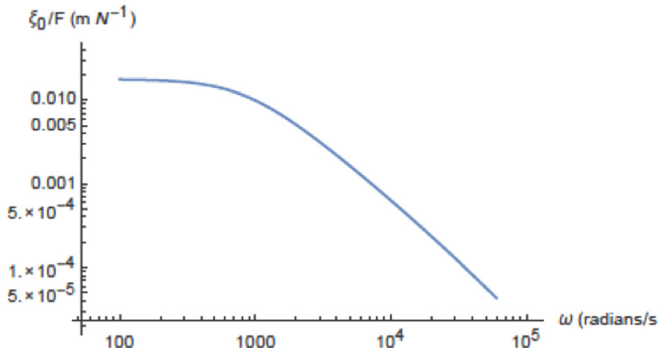

FIG. 13. (Color online) Amplitude of oscillation of a 3 mm sphere per unit force exerted on the medium. $a = 1$ mm, $\mu_1 = 3$ kPa, $\mu_2 = 3$ Pa s.

those suggested by Fig. 12 could make it possible to determine hysteresis levels from very low frequency measurements *in vivo*. In the same way that elastography makes quantitative the information that has historically been obtained by palpation of the liver, low frequency phase measurements could quantitate the information that today is observed qualitatively for edema by palpation.

Oestreicher's impedance raises one final question regarding the temporal characteristics of the pulses used in radiation force elastography. In current clinical devices, the ultrasound pulse that transfers part of its momentum to the tissue has a typical duration on the order of 100 μs, i.e., the frequencies in the driving force are on the order of 10 kHz (60 000 rad s^{-1}). Yet, the maximum of the transition frequency (and maximum response) for typical soft tissues is an order of magnitude smaller [Eq. (10)]. A specific example is shown in Fig. 13. Instead of the diffuse prolate ellipsoid that moves in radiation force elastography, the figure uses an Oestreicher sphere with a radius of 1 mm in a medium with a real shear modulus of 3 kPa and shear viscosity of 3 Pa s. The transition frequency for this system is about 3000 rad s^{-1} ($\sim$500 Hz). Although Oestreicher's solution is for continuous waves, the behavior of the sphere with frequency gives us a semi-quantitative clue to the system's pulse behavior.

Above the transition frequency ω_t, the particle velocity decreases with the reciprocal of the frequency and the particle displacement falls off as the square of the frequency. The energy for a given displacement thus increases as the square of the frequency in that limit. Why not take advantage of the greater efficiency that goes with longer pulses to modulate the driving pulse and in this way obtain a clean dispersion spectrum in the phase velocity? In fact, that has been accomplished with a variety of techniques discussed above (Chen *et al.*, 2004; Chen *et al.*, 2009; Urban *et al.*, 2010; Doherty *et al.*, 2013).

VI. SUMMARY

Through Oestreicher's theory for a translationally oscillating sphere in a viscoelastic medium we see that elastography must deal with complex fields of longitudinal and transverse displacements each of which has a slow wave and a fast wave contribution. The slow wave has the information sought in elastography. The fast wave has no uniquely useful information but, in many cases, is large enough to cause errors in measurements of the slow wave.

At present, clinical wave elastography is limited largely to measurement of phase or group velocity. Because those values are dominated by the real shear modulus of the tissue, they give us a first order estimate of the tissue stiffness. Tissue viscosities are large enough to produce dispersion. Thus, techniques that use high frequency measurements have higher phase velocities than those for lower frequencies. Even so, quantitative elastography has now become an accepted tool for monitoring liver fibrosis.

Viscosity is a qualitatively different physical parameter than stiffness and there is reason to hope that stiffness and viscosity will give us two independent sets of clinically useful data. If we accept the VE model, we can compute the viscosity from dispersion in the measured phase velocity. Using that approach is a qualitative step forward. There is reason, however, to believe that tissue is not a simple VE viscoelastic medium (Carstensen and Parker, 2014; Parker, 2014). This means that both real shear modulus and the real shear viscosity are themselves functions of frequency and we can obtain that information through measurements of both the phase velocity and absorption coefficient at each frequency.

Current measurement techniques can measure phase velocity with reasonable precision. Absorption, however, remains a challenge. Exploring Oestreicher's theory has revealed several promising and complementary routes to measurement of the absorption coefficient: (1) pulse techniques that separate fast and slow waves, (2) computation of the rotation in the displacement field, and (3) impedance techniques.

Not only are the effective real shear moduli and shear viscosities frequency dependent, but in practice their values are functions of strain, i.e., they are nonlinear. Oestreicher assumed tissues to be linear media and all of the discussion in this review is based on that postulate as well. In fact, that may be a reasonable assumption the way that quantitative elastography is practiced today (Liu and Bilston, 2000). However, there is probably no clearer demonstration of the limitations of that assumption than the near universal use of intercostal portals for quantitative measurement of liver stiffness. The static shear strain in caused by a transducer placed on the abdomen appears to alter the small signal (linear) measurement of stiffness and results in interoperator variability. It underlines the fact that liver stiffness is a nonlinear function of shear strain. A number of investigators have been studying nonlinear aspects of shear wave propagation at low frequencies (Catheline *et al.*, 2003; Jacob *et al.*, 2007; Zabolotskaya *et al.*, 2007; Wochner *et al.*, 2008).

The frequency dependent real shear modulus and the frequency dependent shear viscosity each may have their own diagnostic uses particularly if the physical mechanisms responsible for each are elucidated. The same can be said for how each of these parameters is a function of static shear strain. Combined, these data promise to be an extremely powerful diagnostic tool. As technology progresses, elastography may become the "gold standard" to which other tests are referred.

ACKNOWLEDGMENTS

The authors thank Professor David Blackstock, faculty, and students in biomedical ultrasound in the departments of Electrical and Computer, Biomedical, and Mechanical Engineering for valuable discussions. We are indebted to Professor Blackstock for the photograph of Hans Oestreicher taken at the 4th International Congress on Acoustics in Copenhagen, August 1964.

Carstensen, E. L., and Parker, K. J. (**2014**). "Physical models of tissue in shear fields," Ultrasound Med. Biol. **40**, 655–674.

Carstensen, E. L., Parker, K. J., Dalecki, D., and Hocking, D. C. (**2015**). "Biological effects of low frequency shear strain. Part 1. Physical descriptors," Ultrasound Med. Biol. (in press).

Catheline, S., and Benech, N. (**2015**). "Longitudinal shear wave and transverse dilatational wave in solids," J. Acoust. Soc. Am. **137**, EL200–EL205.

Catheline, S., Gennisson, J. L., Delon, G., Fink, M., Sinkus, R., Abouelkaram, S., and Culioli, J. (**2004**). "Measurement of viscoelastic properties of homogeneous soft solid using transient elastography: An inverse problem approach," J. Acoust. Soc. Am. **116**, 3734–3741.

Catheline, S., Gennisson, J. L., and Fink, M. (**2003**). "Measurement of elastic nonlinearity of soft solid with transient elastography," J. Acoust. Soc. Am. **114**, 3087–3091.

Catheline, S., Thomas, J. L., Wu, F., and Fink, M. A. (**1999a**). "Diffraction field of a low frequency vibrator in soft tissues using transient elastography," IEEE Trans. Ultrason. Ferroelectr. Freq. Control **46**, 1013–1019.

Catheline, S., Wu, F., and Fink, M. (**1999b**). "A solution to diffraction biases in sonoelasticity: The acoustic impulse technique," J. Acoust. Soc. Am. **105**, 2941–2950.

Chanaud, R. C. (**2010**). *Tools for Analyzing Sound Sources* (CCR Associates, LLC, Essex, CT), p. 4-2.

Chen, S., Fatemi, M., and Greenleaf, J. F. (**2002**). "Remote measurement of material properties from radiation force induced vibration of an embedded sphere," J. Acoust. Soc. Am. **112**, 884–889.

Chen, S., Fatemi, M., and Greenleaf, J. F. (**2004**). "Quantifying elasticity and viscosity from measurement of shear wave speed dispersion," J. Acoust. Soc. Am. **115**, 2781–2785.

Chen, S., Urban, M. W., Pislaru, C., Kinnick, R., Zheng, Y., Yao, A., and Greenleaf, J. F. (**2009**). "Shearwave dispersion ultrasound vibrometry (SDUV) for measuring tissue elasticity and viscosity," IEEE Trans. Ultrason. Ferroelectr. Freq. Control **56**, 55–62.

Chen, S. G., Sanchez, W., Callstrom, M. R., Gorman, B., Lewis, J. T., Sanderson, S. O., Greenleaf, J. F., Xie, H., Shi, Y., Pashley, M., Shamdasani, V., Lachman, M., and Metz, S. (**2013**). "Assessment of liver viscoelasticity by using shear waves induced by ultrasound radiation force," Radiology **266**, 964–970.

Dahl, J. J. (**2013**). "Acoustic radiation force imaging," in *Emerging Imaging Technologies in Medicine*, edited by M. A. Anastasio and R. La Riviere (CRC Press, Boca Raton, FL), Chap. 13, pp. 201–217.

Deffieux, T., Montaldo, G., Tanter, M., and Fink, M. (**2009**). "Shear wave spectroscopy for quantification of human soft tissues visco-elasticity," IEEE Trans. Med. Imaging **28**, 313–322.

Doherty, J. R., Trahey, G. E., Nightingale, K. R., and Palmeri, M. L. (**2013**). "Acoustic radiation force elasticity imaging in diagnostic ultrasound," IEEE Trans Ultrason Ferroelectr Freq Control **60**, 685–701.

Domire, Z. J., McCullough, M. B., Chen, Q. S., and An, K. N. "Wave attenuation as a measure of muscle quality as measured by magnetic resonance elastography: Initial results," J. Biomech. **42**, 537–540 (**2009**).

Doyley, M. M. (**2012**). "Model-based elastography: A survey of approaches to the inverse elasticity problem," Phys. Med. Biol. **57**, R35–R73.

Gennisson, J. L., and Cloutier, G. (**2006**). "Sol-gel transition in agar-gelatin mixtures studied with transient elastography," IEEE Trans. Ultrason. Ferroelectr. Freq. Control **53**, 716–723.

Gennisson, J. L., Lerouge, S., and Cloutier, G. (**2006**). "Assessment by transient elastography of the viscoelastic properties of blood during clotting," Ultrasound Med. Biol. **32**, 1529–1537.

Greenleaf, J. F., Fatemi, M., and Insana, M. (**2003**). "Selected methods for imaging elastic properties of biological tissues," Ann. Rev. Biomed. Eng. **5**, 57–78.

Jacob, X., Catheline, S., Gennisson, J. L., Barriere, C., Royer, D., and Fink, M. (**2007**). "Nonlinear shear wave interaction in soft solids," J. Acoust. Soc. Am. **122**, 1917–1926.

Liu, Z., and Bilston, L. (**2000**). "On the viscoelastic character of liver tissue: Experiments and modelling of the linear behaviour," Biorheology **37**, 191–201.

Mason, W. P. (**1950**). "Hysteresis losses in solid materials," in *Piezoelectric Crystals and their Application in Ultrasonics* (Van Nostrand, New York), p. 482.

Morse, P. M., and Ingard, K. U. (**1987**). *Theoretical Acoustics* (Princeton University Press, Princeton, NJ), p. 312.

Oestreicher, H. L. (**1951**). "Field and impedance of an oscillating sphere in a viscoelastic medium with an application to biophysics," J. Acoust. Soc. Am. **23**, 707–714.

Oudry, J., Bastard, C., Miette, V., Willinger, R., and Sandrin, L. (**2009**). "Copolymer-in-oil phantom materials for elastography," Ultrasound Med. Biol. **35**, 1185–1197.

Palmeri, M. L., Wang, M. H., Dahl, J. J., Frinkley, K. D., and Nightingale, K. R. (**2008**). "Quantifying hepatic shear modulus *in vivo* using acoustic radiation force," Ultrasound Med. Biol. **34**, 546–558.

Parker, K. J. (**2014**). "A microchannel flow model for soft tissue elasticity," Phys. Med. Biol. **59**, 4443–4457.

Parker, K. J., Doyley, M. M., and Rubens, D. J. (**2011**). "Imaging the elastic properties of tissue: The 20 year perspective," Phys. Med. Biol. **56**, R1–R29.

Sandrin, L., Catheline, S., Tanter, M., Hennequin, X., and Fink, M. (**1999**). "Time-resolved pulsed elastography with ultrafast ultrasonic imaging," Ultrason. Imaging **21**, 259–272.

Sandrin, L., Tanter, M., Gennisson, J. L., Catheline, S., and M. Fink (**2002**). "Shear elasticity probe for soft tissues with 1-D transient elastography," IEEE Trans. Ultrason. Ferroelectr. Freq. Control **49**, 436–446.

Sarvazyan, A. P., Rudenko, O. V., Swanson, S. D., Fowlkes, J. B., and Emelianov, S. Y. (**1998**). "Shear wave elasticity imaging: A new ultrasonic technology of medical diagnostics," Ultrasound Med. Biol. **24**, 1419–1435.

Sarvazyan, A. P., Urban, M. W., and Greenleaf, J. F. (**2013**). "Acoustic waves in medical imaging and diagnostics," Ultrasound Med. Biol. **39**, 1133–1146.

Schmitt, C., Hadj Henni, A., and Cloutier, G. (**2011**). "Characterization of blood clot viscoelasticity by dynamic ultrasound elastography and modeling of the rheological behavior," J. Biomech. **44**, 622–629.

Sinkus, R., Tanter, M., Xydeas, T., Catheline, S., Bercoff, J., and Fink, M. (**2005**). "Viscoelastic shear properties of *in vivo* breast lesions measured by MR elastography," Magn. Reson. Imaging **23**, 159–165.

Urban, M. W., Chen, S. G., and Greenleaf, J. F. (**2009**). "Error in estimates of tissue material properties from shear wave dispersion ultrasound vibrometry," IEEE Trans. Ultrason. Ferroelectr. Freq. Control **56**, 748–758.

Urban, M. W., Fatemi, M., and Greenleaf, J. F. (**2010**). "Modulation of ultrasound to produce multifrequency radiation force," J. Acoust. Soc. Am. **127**, 1228–1238.

Urban, M. W., and Greenleaf, J. F. (**2009**). "A Kramers-Kronig-based quality factor for shear wave propagation in soft tissue," Phys. Med. Biol. **54**, 5919–5933.

Urban, M. W., Nenadic, I. Z., Mitchell, S. A., Chen, S., and Greenleaf, J. F. (**2011**). "Generalized response of a sphere embedded in a viscoelastic medium excited by an ultrasonic radiation force," J. Acoust. Soc. Am. **130**, 1133–1141.

Wochner, M. S., Hamilton, M. F., Ilinskii, Y. A., and Zabolotskaya, E. A. (**2008**). "Cubic nonlinearity in shear wave beams with different polarizations," J. Acoust. Soc. Am. **123**, 2488–2495.

Zabolotskaya, E. A., Ilinskii, Y. A., and Hamilton, M. F. (**2007**). "Nonlinear surface waves in soft, weakly compressible elastic media," J. Acoust. Soc. Am. **121**, 1873–1878.